Automated Landing of an Intelligent Unmanned Aerial Vehicle in Crosswind Conditions using Total Energy Control

C.T. Le Roux
Department of Electrical & Electronic Engineering
Stellenbosch University
Stellenbosch, South Africa
Email: cornelusleroux@gmail.com

J.A.A. Engelbrecht
Department of Electrical & Electronic Engineering
Stellenbosch University
Stellenbosch, South Africa
Email: jengelbr@sun.ac.za

***Abstract*—This paper presents the development, implementation and verification of a flight control system for the automated landing of an intelligent unmanned aerial vehicle (UAV) in crosswind conditions.**

There is an increasing number of commercial opportunities for UAVs in business, agriculture, industry and mining, the emergency services and security services. The major barrier to commercialisation of UAVs is the certification process, where automated take-off and landing is a key feature required.

The automated landing system presented in this paper uses a longitudinal control system based on the total energy control system (TECS), and a lateral control system that combines a heading and guidance controller with a cross-track error controller. A software state machine is used to advance the flight control system through the different stages of the automated landing. The TECS architecture allows the airspeed and flight path angle to be decoupled, while the Cross-Track Controller uses a limited integrator to drive the cross-track error to zero in the presence of crosswind.

The automated landing system is implemented on a UAV with an on-board computer, sensors and actuators, and is verified in simulation and with practical flight tests. The hardware simulation results show that the UAV is able to land autonomously in crosswinds up to 3.6 metres per second, with a landing accuracy of 3.50 metre in-track and 0.12 metre cross-track.

I. Introduction

There is an increasing number of commercial opportunities for UAVs in business (aerial photography, speed courier services), agriculture (surveying, crop inspection, crop dusting, farm security), industry and mining (power line inspection, prospecting), the emergency services (disaster monitoring, delivery of emergency supplies, firefighting) and security services (surveillance, policing). However, a major barrier to the commercialisation of unmanned aircraft is the certification process. Before UAVs can be operated in civil airspace, they must first pass a rigorous certification process to prove that they will operate safely. One of the key enabling technologies required for the certification and eventual integration of intelligent unmanned aircraft into commercial airspace is automated take-off and landing.

Autonomous landing systems are currently researched globally by various institutions for different applications. Cho et al. [4] developed a system using only a single-antenna GPS receiver, implementing differential GPS (DGPS) for increased accuracy in position information. The only extra sensor used was for airspeed via the pitot tube, as accurate airspeed measurements are very important during the landing phase. López et al. [8] presented a paper on the differences between H_∞ and quantitative feedback theory techniques that should be robust against wind disturbances and control the altitude accurately. They found that controllers designed by both techniques guaranteed robust stability and attenuated high frequency noise due to sensors supplying suitable control signals. Masuko et al. [9] opted to use visual feedback, using a small Linux ARM computer running OpenCV. The high velocity of the aircraft resulted in blurred images taken by the camera which could not be processed fast enough to ensure safe landing.

Akmeliawati and Mareels [1] presented a non-linear energy-base control method (NEM) based on passivity-based control techniques similar to TECS. The difference between their technique from TECS was that the non-linearity of the system dynamics were directly taken into account, where the aircraft dynamics are expressed in Euler-Lagrange equations of motion derived from the energy equations. In [2], they extended the NEM technique by further exploiting the inherent time scales of the dynamics using a singular perturbation technique to simplify the overall design. The aircraft is treated as a single point mass while disregarding the fast pitch and elevator dynamics. The system conforms to the Lyapunov stability criteria, and good stability and performance were achieved during Monte Carlo simulations. Looye and Joos [7] used multi-objective optimisation to design a controller with the purpose to synthesise the free parameters (gains, time-constants) in these controller functions by using parameter weighting, sequentially expanded to the simultaneous optimisation of all functions. The system was successfully flight tested, however the glide slope and disturbance rejection criteria did not work to full satisfaction.

This paper focus on a simpler design using accurate sensors, mainly the NovAtel DGPS system operating in ALIGN™ mode to provide very accurate position measurements. The

 ISBN: 978-0-7972-1533-7

Fig. 1. Photograph of a Phoenix Trainer 60, the model aircraft used in this project.

simpler design introduces fewer modelling errors and speeds up the design process and testing iterations while keeping functionality. The end goal of the project is to make the UAV capable of landing on a moving platform, such as a naval vessel.

II. Mathematical Models

To design and test the system in simulation, a model is required representative of the aircraft, avionics, and environmental factors. The models used are discussed below.

A. Aircraft

The aircraft model used is explained thoroughly in [5] using the standard North-East-Down convention for inertial space and Euler-3-2-1 angle conversions. The model includes

1) forces and moments, which include the aerodynamic, engine/thrust, and gravitational models; and
2) six degrees of freedom equations of motion, which includes the kinetic and kinematic models.

The model aircraft used is a Phoenix Trainer 60, modified with custom sensors and actuators. The aircraft will be flown by the autopilot system, but a safety pilot can assume control if required. An illustration of the vehicle is shown in Fig. 1.

B. Wind Model

With the focus on landing during windy conditions, the Dryden and Von Kármán wind models, as presented in military standards [10] and [11], were implemented in simulation to more accurately reflect wind conditions and the effect thereof on the aircraft. These include models for

1) turbulence: the irregular forces and moments acting on the aircraft caused by chaotic winds;
2) shear: the variation in wind velocity caused by difference in altitude; and
3) gusts: shorts bursts of high velocity wind.

C. Sensor Models

To reflect inaccuracies in the on-board measurements systems, models of the sensors used on-board the model aircraft are implemented to include noise on the measurements they provide. These include models for

1) 3-axis magnetometer;

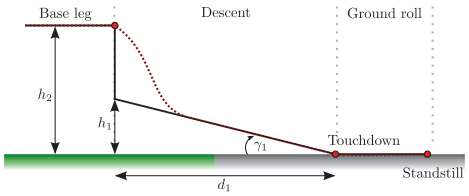

Fig. 2. Side view of the flight path during the different states of landing.

2) 3-axis gyroscope;
3) 3-axis accelerometer;
4) global positioning system (GPS); and
5) pressure sensor (pitot tube).

III. Control System Design

The design of the controllers has seen continuous adaptation throughout the project. The controllers implemented are explained in their respective sections below.

A. Landing Controller

The airfield where the system will be flight tested has obstacles in the runway path that may threaten safe flying conditions. To circumvent this, a flight path is proposed as illustrated in Fig. 2. After flying at $h_2 = 20$ m altitude until sufficient obstacle clearance is achieved, a ramp starting at a lower altitude will be commanded at a flight path angle of $\gamma_1 = 3.5°$ until the touchdown point. This sequence is activated $d_1 = 200$ m before the touchdown point so that the ramp initial altitude is $h_1 = 12.23$ m. This method is proposed because the aircraft cannot be trimmed to a much steeper angle while keeping low airspeed. The aircraft is thus allowed to reduce altitude as fast as possible to reach the region in which it can be successfully trimmed to the landing conditions. Since the end goal of the project is landing on a moving platform, the flare procedure is omitted and the landing executed similarly to real pilot touchdowns when landing on naval vessels. Upon touchdown, a safety pilot will assume control of the aircraft and bring it to a halt as runway taxiing is outside the scope of this project.

The trim airspeed was chosen at 16 m/s, which is well above the aircraft's stall speed of approximately 12 m/s and therefore deemed safe. The low glide slope may reduce landing accuracy as shown in predecessors of this project, [3] and [13].

Two other methods are also proposed to apply course correction for both a stationary and moving touchdown point. The first uses proportional navigation techniques to supply longitudinal reference signals to regulate the line-of-sight angle between the aircraft and the touchdown point. The other uses touchdown point estimation and trigger re-planning of the glide path when the error would be out of predefined bounds. As the system is still under development, these techniques will not be discussed further in this paper.

B. Longitudinal Controller

The concept of an energy controller was pioneered and patented by [6] in 1985. The main purpose of this controller is

 ISBN: 978-0-7972-1533-7

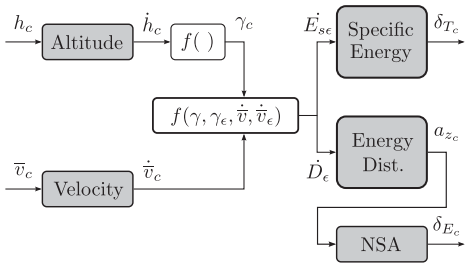

Fig. 3. Simplified Total Energy Control System concept with the pitch control inner loops replaced by a Normal Specific Acceleration Controller.

to balance the kinetic and potential energy of the aircraft with an integrated and simplified control system architecture, using the throttle to control the aircraft's total energy error and the elevator to control the energy distribution error between flight path and airspeed. The explanation below is illustrated by the simplified block diagram of the TECS architecture in Fig. 3, with all parameters designed in a heuristic fashion.

The aircraft's total energy E can be expressed by

$$E = mgh + \frac{1}{2}mV^2 \tag{1}$$

which is the sum of the potential and kinetic energy components, where m is the aircraft's mass, g is the gravitational acceleration, h is the altitude of the aircraft, and V is the velocity. By assuming a constant weight of $W = mg$, Eq. 1 can be rewritten and time-derived to form

$$\dot{E} = W\left(\dot{h} + \frac{V\dot{V}}{g}\right) \tag{2}$$

Using the small angle approximation, the flight path angle γ can be calculated as

$$\gamma = \frac{\dot{h}}{V} \tag{3}$$

Substituting Eq. 3 into Eq. 2 and scaling the result by V, a velocity normalised energy rate equation is obtained, yielding

$$\frac{\dot{E}}{V} = W\left(\gamma + \frac{\dot{V}}{g}\right) \tag{4}$$

This reveals that, at a given airspeed, the rate of change of the aircraft's energy is dependant only on the flight path angle and longitudinal acceleration.

The second law of Newton, $F = ma$, is used to express the longitudinal motion of the aircraft as

$$\frac{W}{g}\dot{V} = T - D + W\sin\gamma \tag{5}$$

where T is the total thrust applied and D is the total drag. By again assuming a small flight path angle, the equation can be rewritten as

$$W\left(\gamma + \frac{\dot{V}}{g}\right) = T - D \tag{6}$$

This resembles Eq. 4, concluding that the rate of change of the aircraft's energy is proportional to the difference between thrust and drag. The required thrust can then be written as

$$T_{req} = W\left(\gamma + \frac{\dot{V}}{g}\right) + D \tag{7}$$

$$= \frac{\dot{E}_s}{V} + D \tag{8}$$

where $\dot{E}_s$ is the specific energy rate of the aircraft.

At a specific thrust level, it is possible to exchange flight path angle and acceleration by only using the elevator. To drive the aircraft's current flight path angle and longitudinal acceleration towards desired reference values, it becomes apparent that a flight path and speed control concept is obtained in the form of total specific energy rate, given as

$$\dot{E}_{s\epsilon} = \gamma_\epsilon + \frac{\dot{V}_\epsilon}{g} \tag{9}$$

where subscript ϵ denotes the error between the reference and measured signal values. The elevator is to be driven until the energy rate distribution error

$$\dot{D}_\epsilon = -\gamma_\epsilon + \frac{\dot{V}_\epsilon}{g} \tag{10}$$

relative to the target flight path and acceleration is zero. The specific energy rate error is used directly in the computation of the thrust command δ_T, and the energy rate distribution error is similarly applied to the elevator command δ_E.

In most cases, it is desired to command the aircraft altitude and airspeed rather than the flight path angle and acceleration. To realise this, two outer loops of both proportional control are implemented in the design with gains K_h and K_v for altitude and airspeed which produce climb rate and acceleration commands, respectively. The climb rate command can also be given directly instead of being determined from the altitude controller, resulting in three operational modes to change aircraft altitude—flight path angle, climb rate or direct altitude commands. The gains K_v and K_h are selected to have equal values to provide identical altitude and airspeed dynamics. In essence, they determine the error decay time constants in the altitude and airspeed responses. Using these control mechanisms, the altitude and speed errors are now scaled in relative energy terms.

In the classic TECS, the result of the energy distribution rate controller is used as a pitch angle command, which feeds a Pitch Angle Controller with proportional gain K_θ. This in turn feeds a Pitch Rate Damper with proportional gain $K_{\dot{\theta}}$, which finally produces the elevator command. In addition to the default TECS, a climb rate feed forward was added in the climb rate loop to ensure that the correct sink rate was maintained upon landing. The Pitch Angle Controller and Pitch Rate Damper loops were replaced by a Normal Specific Acceleration (NSA) Controller which more directly controls the angle of attack of the aircraft. The proportional segments of the controllers were also fed from the error signals rather

 ISBN: 978-0-7972-1533-7

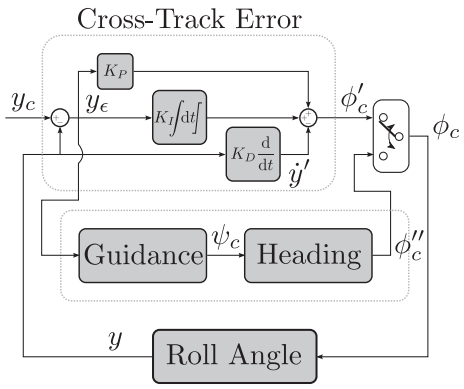

Fig. 4. Simplified block diagram of the lateral controllers with the Cross-Track Error Controller expanded and the Dutch Roll Damper omitted.

than pure measurements to improve damping. The simulation results are discussed in Sec. IV.

Advantages of the TECS are that there are now a multitude of possible reference signals which all share the same architectural inner loops, and that a change in airspeed reference does not significantly influence the flight path angle and vice versa. A clear disadvantage is the challenging design method, although this was overcome by separating the terms of the specific energy and energy distribution signals, treating one as the reference and the other as a disturbance, allowing for a root locus design.

C. Lateral Controllers

The navigation system uses a waypoint structure of connected straight line segments. To allow for curved turns, which should yield a better transient response, the aircraft was guided to a new destination waypoint before reaching the current one. This caused a problem in the Cross-Track Controller, as the proportional part will overpower the derivative part at the chosen trim velocity, causing a turn in the wrong direction. To correct this problem, it was decided to implement two controllers which would run in tandem—a less aggressive Heading and Guidance Controller for when the aircraft is far from the waypoint track, and a more aggressive Cross-Track Controller for when the cross-track error is small. A simplified block diagram of the combined controllers is shown in Fig. 4. The strategy of the controllers are discussed in their respective sections below. All gains were designed using the root locus method. Simulation results are discussed in Sec. IV.

1) Dutch Roll Damper: The Dutch Roll Damper simply feeds back the aircraft's yaw rate though a high-pass filter with a proportional gain, which feeds the rudder to produce artificial damping. The high-pass filter constant is chosen as to not prevent constant turn rate motions. This controller is common to the Heading and Guidance and the Cross-Track Controllers.

2) Roll Angle Controller: The Roll Angle Controller (RAC) is a simple proportional-integral controller that generates an aileron command given a roll angle error. It is designed for optimal damping and is also common to the Heading and Guidance and the Cross-Track Controllers, with both these controllers feeding the RAC directly.

3) Heading and Guidance Controllers: The Heading and Guidance Controller is a somewhat slow controller and is used to guide the aircraft back to the current waypoint track when very far away. The Heading Controller inner loop generates a roll angle command ϕ_{ref} proportional to the heading error ψ_ϵ. The roll angle command then causes a heading rate, causing the heading to change. The heading error is wrapped to always act on the smallest error angle to prevent turning in an inefficient direction. The Guidance Controller outer loop generates a heading angle command ψ_{ref} proportional to the cross-track error y_ϵ. The heading angle command then causes a cross-track error rate, causing the cross-track error to reduce.

4) Cross-Track Error Controller: The Cross-Track Controller feeds the RAC directly, thereby reducing the time-scale separation which is present in the Heading and Guidance Controller, allowing for a significantly faster transient response as well as zero steady-state error. Both these controllers supply the RAC with a roll angle reference, and a state machine switches between the two.

This controller is designed as a proportional-derivative controller, but has an additional limited integrator included. The commands generated are:

1) proportional, obtained by multiplying the cross-track error y_ϵ by a factor K_P;
2) derivative, obtained by multiplying the cross-track rate $\dot{y}$ by a factor K_D. The cross-track rate is used rather than the error rate to avoid a signal spike when changes in reference are given; and
3) integral, obtained by multiplying the integral of the cross-track error y_ϵ by a factor K_I. The bias in the roll angle measurement causes a steady-state error in the roll angle control which manifests as a lateral acceleration disturbance from the viewpoint of the Cross-Track Error Controller. The limited integrator in the Cross-Track Controller rejects this constant disturbance, achieving zero steady-state error in cross-track.

The produced roll angle reference, the sum of the three commands, are then fed directly to the RAC.

Switching from the Heading and Guidance Controller to the Cross-Track Error Controller takes place when the aircraft is within a certain distance from the track. However, if the aircraft moves too far away from the track of whatever reason, control is given back to the Heading and Guidance Controller to return to the correct course.

IV. Non-Linear Simulation

To evaluate the system performance in a rapid-testing environment, software-in-the-loop (SIL) features were added to the simulation to allow running the same code that would be executed on the on-board micro-controller unit. After initial testing showed positive results, the system was implemented on the physical hardware to allow for hardware-in-the-loop (HIL) simulations.

 ISBN: 978-0-7972-1533-7

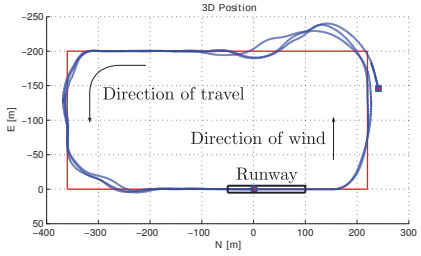

Fig. 5. Dual-mode lateral controller response on the intended waypoint track.

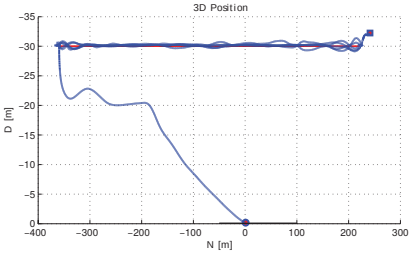

Fig. 6. TECS altitude regulation and landing sequence.

In the simulation, the on-board computer and extended Kalman filter are initialised on the touchdown point on the runway, after which a manual take-off is performed. The autopilot is activated and go-arounds are performed to test the regulation of altitude, airspeed and track navigation. After sufficient go-arounds, the landing command is given and the aircraft continues to fly the circuit with the landing sequence started when the final waypoint and approach points are reached. The aircraft follows the landing states and touches down on the runway as illustrated in Figs. 5–6. It was subjected to turbulence and an east-to-west crosswind of 10 km/h, which is over 17% of the flight speed.

TECS regulates the altitude to within a 1.0 m error, barely losing altitude when rolling at angles of up to 30°. However it does increase the airspeed by up to 10%, exchanging potential energy for kinetic energy. For the straight legs, it can be seen that the cross-track error is reduced to zero shortly after the system is switched from the Heading and Guidance to the Cross-Track Error Controller. The early waypoint switching method works to satisfaction, providing a better transient response similar to the non-linear guidance method as proposed by Park [12] and implemented by Alberts [3]. A noticeable effect is observed when the aircraft is subjected to a tailwind, which causes loss of lift force and increases waypoint track overshoot.

The simulations showed 95% confidence in landing within 3.50 m in-track and 0.12 m cross-track, which is 1.75 and 0.06 wingspan, respectively. Although the longitudinal accuracy is good for landing on a fixed runway or large naval vessel, it still needs improvement to obtain an accuracy better than 0.5 wingspan to land on a moving platform during a practical flight test. To improve the longitudinal accuracy, the landing strategy will be revised and complemented by proportional navigation techniques. The lateral accuracy is exceptional for such a small aircraft in light wind conditions and do not need any further improvement.

V. Conclusion

This paper presented the implementation of concepts that would allow a UAV to successfully land with acceptable accuracy in crosswind conditions using total energy control and an aggressive cross-track control system.

A modified landing sequence, controlled by a software state machine, was presented to allow for a flight-testable landing on a runway with hazards. Longitudinal performance in TECS shows good control during the circuit navigation and landing phases, even with high roll angle references given by the lateral controllers. Upon landing, the system does achieve the correct sink rate as well as a positive pitch angle. Lateral performance with the combination of the Heading and Guidance Controllers and the Cross-Track Controller can be considered exceptional and further improvements are not required, as the landing error is almost zero under acceptable disturbances.

Further work would include attempting to increase longitudinal accuracy by incorporating proportional navigation or estimation and re-planning methods. This is not only beneficial to a runway landing, but also to a landing where the touchdown point is moving. The system is currently being subjected to further HIL simulations in preparation for flight tests, which should yield more results on practical feasibility.

References

[1] R. Akmeliawati, I. Mareels, *Nonlinear Energy-based Control Method for Aircraft Dynamics*. Decision and Control, 2001. Proceedings of the 40th IEEE Conference on, Pages 658–663, 2011.

[2] R. Akmeliawati, I. Mareels, *Nonlinear Energy-Based Control Method for Aircraft Automatic Landing Systems*. Control Systems Technology, IEEE Transactions on, Vol. 18, Pages 871–884, 2010.

[3] F. N. Alberts, *Accurate Autonomous Landing of a Fixed-Wing Unmanned Aerial Vehicle*. Stellenbosch University, 2012.

[4] A. Cho, J. Kim, S. Lee, S. Choi, B. Lee, B. Kim, N. Park, D. Kim, C. Kee, *Fully Automatic Taxiing, Takeoff and Landing of a UAV Using a Single-Antenna GPS Receiver Only*. Control, Automation and Systems, 2007. International Conference on, Pages 821–825, 2007.

[5] M. V. Cook, *Flight Dynamics Principles*, 3nd ed. Elsevier Ltd., 2007.

[6] A. A. Lambregts, *Total Energy Based Flight Control System*, US Patent Nr. 6062513. The Boeing Company (Seattle, WA), 1985.

[7] G. Looye, H.D. Joos, *Design of Autoland Controller Functions with Multi-Objective Optimization*. AIAA Guidance, Navigation, and Control Conference and Exhibit, 2002.

[8] J. Lopéz, R. Dormiro, J. P. Gómez, *A Fully Autonomous UAV Landing Controller Synthesis - QFT and H_∞ Technique Comparison*, 3nd ed. Proceedings of the Institution of Mechanical Engineers, Part G: Journal of Aerospace Engineering 2012, Pages 281–293, 2011.

[9] K. Masuko, I. Takahashi, S. Ogawa, W. Meng-Hung, A. Oosedo, T. Matsumoto, K. Go, F. Sugai, A. Konno, M. Uchiyama, *Autonomous Takeoff and Landing of an Unmanned Aerial Vehicle*. System Integration, International Symposium on, Pages 248–253, 2010.

[10] United States Department of Defense, *MIL-HDBK-1797*. United States Department of Defense, 1997.

[11] United States Department of Defense, *MIL-F-8785C*. United States Department of Defense, 1980.

[12] S. Park, J. Deyst, J. P. How, *A New Nonlinear Guidance Logic for Trajectory Tracking*. In AIAA Guidance, Navigation, and Control Conference and Exhibit, Pages 1–16, 2004.

[13] S. J. A. Smit, *Autonomous Landing of a Fixed-Wing Unmanned Aerial Vehicle using Differential GPS*. Stellenbosch University, 2013.